

Copper(II) Complexes with Unusual Axial Phenolate Coordination as Structural Models for the Active Site in Galactose Oxidase: X-ray Crystal Structures and Spectral and Redox Properties of [Cu(bpnp)X] Complexes

Mathrubootham Vaidyanathan, Rathinam Viswanathan, Mallayan Palaniandavar,*
T. Balasubramanian, P. Prabhakaran, and Thomas P. Muthiah

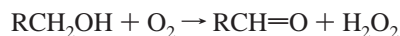
Department of Chemistry, Bharathidasan University, Tiruchirappalli 620 024, India

Received December 15, 1997

The crystal structures of [Cu(bpnp)(SCN)]·NH₄SCN (**1**), [Cu(bpnp)(CH₃COO)]·CH₃OH·C₈H₁₀ (**2**), and [Cu(bpnp)ClO₄] (**3**) [Hbpnp = 2-(bis(pyrid-2-ylmethyl)aminomethyl)-4-nitrophenol] reveal a distorted square pyramidal geometry around Cu(II) with an unusual axial coordination of phenolate. The mononuclear complex [Cu(bpnp)(SCN)]·NH₄SCN crystallizes in the triclinic space group *P* $\bar{1}$ with *a* = 10.796(2) Å, *b* = 10.804(2) Å, *c* = 12.559(2) Å, α = 71.38(1)°, β = 72.68(1)°, γ = 61.69(1)°, and *Z* = 2. The mononuclear acetate [Cu(bpnp)(CH₃COO)]·CH₃OH·C₈H₁₀ crystallizes in the triclinic space group *P* $\bar{1}$ with *a* = 10.480(6) Å, *b* = 12.116(4) Å, *c* = 12.547(3) Å, α = 98.77(3)°, β = 113.37(3)°, γ = 100.78(3)°, and *Z* = 2. The binuclear perchlorate complex crystallizes in the monoclinic space group *C*2/*c* with *a* = 13.417(3) Å, *b* = 20.095(2) Å, *c* = 16.401(2) Å, α = 102.21(2)°, and *Z* = 8. The coordination plane in all these complexes is comprised of the tertiary amine and two pyridine nitrogens. The fourth equatorial position is occupied by SCN[−]/CH₃COO[−] in the mononuclear complexes but by the coordinated phenolate ion from the adjacent molecule in the perchlorate complex, resulting in its dimerization. The unusual occupation of phenolate ion in the axial site is possibly due to the steric constraint at copper imposed by the 5,5,6-chelate ring sequence. The thiocyanate/acetate coordination geometry is reminiscent of the active site of the radical copper enzyme galactose oxidase (GOase) with an axial phenolate and equatorial SCN[−]/CH₃COO[−] ligands. Further, the present complexes exhibit several spectral features also similar to this enzyme. The addition of chloride or thiocyanate or acetate ions dissociates the dimeric structure of the perchlorate complex to produce the corresponding monomeric derivatives. The study of the interaction of the acetate complex with N₃[−] and CN[−] ions provide insight into the anion binding properties of the enzyme. The sensitivity of the acetate complex to protons suggests the facile dissociation of the axial phenolate which then acts as a base to bind to protons. The implication of this reaction to the GOase mechanism is discussed.

Introduction

Galactose oxidase (GOase) is an extracellular copper containing enzyme secreted by the fungus *Dactylium dendroides*, that catalyzes the two-electron oxidation of primary alcohols by molecular oxygen yielding the corresponding aldehyde and H₂O₂:¹



It exhibits two-electron oxidation, despite having only a single monomeric copper in the active site and the unusual catalysis has been ascribed^{2,3} to a tyrosyl free radical incorporated into the redox unit during the catalytic cycle. The complete regioselectivity and broad substrate specificity have made this enzyme interesting for potential applications in organic synthesis and as a model for synthetic alcohol oxidation catalysts.³ A

recent report⁴ on the crystal structure of this enzyme reveals Cu(II) located in a square pyramidal environment. The amino acids Tyr-272, His-496, and His-581 and an acetate ion form an almost perfect square with respective distances from copper of 1.94, 2.11, 2.15, and 2.27 ± 0.15 Å and the axial ligand Tyr-495 is at 2.65 Å from copper. An interesting feature of this structure is a covalent thioether bond formed between a cystein sulfur atom and an aromatic carbon atom of the equatorial tyrosinate ligand.

To establish the structural and spectroscopic consequences of phenolate donors in this enzyme, we initiated a study of monomeric copper(II) complexes containing phenolate and imidazole donors as structural models toward GOase. Bereman et al. have studied⁵ a number of copper(II) complexes of tridentate ligands with various donor atoms in an attempt to duplicate the unusual reactivity patterns and accompanying spectral changes of the copper(II) center in GOase upon anion binding. In fact one of these complexes^{5d} correctly predicted

* To whom all correspondence should be addressed. E-mail: palani@bdu.ernet.in.

- (1) (a) Avigad, G.; Amaral, D.; Asensio, C.; Horecker, B. *J. Biol. Chem.* **1962**, 237, 2736. (b) Whittaker, M. M.; Whittaker, J. W. *J. Biol. Chem.* **1988**, 263, 6074. (c) Whittaker, M. M.; Whittaker, J. W. *Biophys. J.* **1993**, 64, 762. (d) Klinman, J. P. *Chem. Rev.* **1996**, 96, 2541.
- (2) Whittaker, M. M.; DeVito, V. L.; Asher, S. A.; Whittaker, J. W. *J. Biol. Chem.* **1989**, 264, 7104.
- (3) Whittaker, J. W. In *Bioinorganic Chemistry of Copper*; Karlin, K. D., Tyeklar, Z., Eds.; Chapman Hall: New York, 1993; pp 447–458.

- (4) Ito, N.; Philips, S. E. V.; Stevens, C.; Ogel, Z. B.; McPherson, M. J.; Keen, G. N.; Yadav, K. D. S.; Knowles, P. F. *Nature (London)* **1991**, 350, 87.
- (5) (a) Giordano, R. S.; Bereman, R. D.; Kosman, D. J.; Ettinger, M. J. *J. Am. Chem. Soc.* **1974**, 96, 1023. (b) Winkler, M. E.; Bereman, R. D. *J. Am. Chem. Soc.* **1980**, 102, 6224. (c) Marwedel, B. J.; Kosman, D. J.; Bereman, R. D.; Kurland, R. J. *J. Am. Chem. Soc.* **1981**, 103, 2842. (d) Bereman, R. D.; Shields, G. D.; Dorfman, J. R.; Bordner, J. *J. Inorg. Biochem.* **1983**, 19, 75.

the active site structure of the enzyme even before its crystal structure was published. In a recent paper we reported⁶ the X-ray crystal structure and spectroscopic and electrochemical study of the mononuclear complex $[\text{Cu}(\text{bnp})\text{Cl}]$ [$\text{Hbnp} = 2\text{-(bis(pyrid-2-ylmethyl)aminomethyl)-4-nitrophenol}$]. This complex is the first one to contain an unusually axially coordinated phenolate and mimic the axial $\text{Cu(II)}\text{--phenolate}$ bond in the inactive GOase.⁶ On the other hand, the phenolate group is coordinated equatorially rather than axially in the analogous model complexes reported by Fenton et al.⁷ Whittaker et al. investigated the structures of several mononuclear copper(II) complexes⁸ derived from the simple polyamine $N,N,N',N'',N'''\text{-pentamethyldiethylenetriamine}$ and $p\text{-cresol}$, 2-methylsulfanyl, or 2-methylsulfanyl- $p\text{-cresol}$ in order to closely mimic the cystein-modified tyrosinate in the protein species. Much progress^{9,10} toward understanding the nature of the active sites of the enzymes has been now made by the characterization and reactions of several $\text{Cu(II)}\text{--phenoxy}$ radical species. However, appropriate and closely mimicking mononuclear model complexes and their derived metal-phenoxyl radical species stabilized by ligands are still lacking.

It has been established³ that many features of the chemistry of GOase is altered by the interaction of the enzyme with exogenous anions. Thus the anion binding to the inactive enzyme results in a decrease in intensity and a shift to higher energy of the ligand field band; further, the elimination of the 440 nm tyrosine-to- Cu(II) CT band takes place for the inactive but not for the active enzyme.³ The binding of exogenous ligands modulates the basicity of the axial tyrosine phenolate by pseudorotation, permitting the phenolate to serve as a general base in catalysis.^{9b,11} Further, such metal-exogenous ligand interactions can clearly affect the radical site interactions, perhaps even modulating the metal-radical coupling³ and related redox characteristics of the active enzyme. The presence of two copper(II) coordination sites, one axial and one equatorial

for exogenous ligands has been established using ^{19}F NMR^{5c} and EPR studies^{5c,d} of CN^- and F^- binding to the enzyme. However, the coordination chemistry of exogenous ligand binding to enzyme is still not completely and clearly elucidated. To duplicate and further understand the anion interactions in the inactive enzyme and the unique spectral changes accompanying it we have now determined the crystal structures of a series of $[\text{Cu}(\text{bnp})\text{X}]$ complexes [$\text{X}^- = \text{ClO}_4^-$, SCN^- , CH_3COO^-] and probed the effect of incorporating different anions on the coordination geometry as well as the electronic and EPR spectral and redox properties. The acetate complex has been prepared with an aim to simulate the basal interactions found at the copper site of the enzyme.¹² Thus the present study, in comparison with model complexes having no axial but equatorial $\text{Cu(II)}\text{--phenolate}$ bond,⁷ would be expected to yield valuable information on the electronic interactions in the inactive form of GOase. As in the chloride complex, the present series of complexes contain the novel axially coordinated phenolate ion.

Experimental Section

Reagents and solvents used in this study were commercial products of the highest available purity and were purified by the standard methods. Elemental analyses for the complexes were performed at Central Drug Research Institute, Lucknow, India. The reflectance and solution spectra were recorded on a Hitachi U-3400 double beam UV-vis-NIR spectrophotometer. EPR spectra were obtained on a Varian E-112 X-band spectrometer, the field being calibrated with diphenylpicrylhydrazyl (DPPH). The values of g_0 and A_0 were measured at ambient temperature and those of g_{\parallel} and A_{\parallel} at 77 K.

Cyclic voltammetry and differential pulse voltammetry on a platinum sphere electrode were performed at $25.0 \pm 0.2^\circ\text{C}$. A three-electrode cell configuration was used. The reference electrode was Ag(s)/AgNO_3 (0.01 M), tetra- n -hexylammonium perchlorate (0.1 M) in acetonitrile. The temperature of the electrochemical cell was maintained at $25 \pm 0.2^\circ\text{C}$ by a cryocirculator (Hakke D8 G). The solutions were deoxygenated by bubbling research grade nitrogen. The instrument utilized included a EG&G PAR 273 potentiostat/galvanostat and an IBM PS-2 computer. EG&G M270 software was employed to carry out the experiments and to acquire the data.

Syntheses. The ligand 2-(bis(pyrid-2-ylmethyl)aminomethyl)-4-nitrophenol (Hbnp) was obtained as a syrup.¹³

$[\text{Cu}(\text{bnp})(\text{SCN})]\cdot\text{NH}_4\text{SCN}$ (1). The complex prepared as reported^{6b} already was dissolved in methanol, a small amount of ammonium thiocyanate added, and the solution kept standing for a few days. The dark green crystals (1) obtained were suitable for X-ray diffraction. Anal. Calcd for $\text{C}_{21}\text{H}_{21}\text{N}_7\text{CuO}_3\text{S}_2$: C, 46.10; H, 3.87; N, 17.92. Found C, 46.36; H, 4.08; N, 18.25.

$[\text{Cu}(\text{bnp})(\text{O}_2\text{CCH}_3)]\cdot\text{CH}_3\text{OH}\cdot\text{C}_8\text{H}_{10}$ (2). To the ligand Hbnp (1 mmol) was added Et_3N (1 mmol, 0.1 g) followed by $\text{Cu}(\text{CH}_3\text{COO})_2\cdot\text{H}_2\text{O}$ (1 mmol, 0.2 g) in methanol. The solution was stirred well to obtain a dark green solution a small amount of $p\text{-xylene}$ added and then cooled for a week in a refrigerator to obtain fine green crystals (2) suitable for X-ray diffraction.¹² Anal. Calcd for $\text{C}_{30}\text{H}_{34}\text{N}_4\text{CuO}_6$: C, 59.05; H, 5.62; N, 9.18. Found: C, 58.85; H, 5.82; N, 9.29.

$[\text{Cu}(\text{bnp})]_2(\text{ClO}_4)_2\cdot 2\text{H}_2\text{O}$ (3). The dimeric complex was prepared as reported earlier.^{6b} A solution of this complex in methanol on standing at room temperature gave shiny blue crystals (3) suitable for X-ray analysis. Anal. Calcd for $\text{C}_{19}\text{H}_{17}\text{N}_4\text{CuO}_7\text{Cl}$: C, 44.54; H, 3.34; N, 10.94. Found: C, 44.75; H, 3.34; N, 9.94.

Crystallographic Data Collection and Structure Analysis. Crystals showing nice extinction under a polarizing microscope were used

- (6) (a) Rajendran, U.; Viswanathan, R.; Palaniandavar, M.; Lakshminarayanan, M. *J. Chem. Soc., Dalton Trans.* **1992**, 3563. (b) Uma, R.; Viswanathan, R.; Palaniandavar, M.; Lakshminarayanan, M. *J. Chem. Soc., Dalton Trans.* **1994**, 1219.
- (7) (a) Adams, H.; Bailey, N. A.; Fenton, D. E.; He, Q.-Y.; Ohba, M.; Okawa, H. *Inorg. Chim. Acta* **1994**, 215, 1. (b) Adams, H.; Bailey, N. A.; Rodriguez de Barbarin, C. O.; Fenton, D. E.; He, Q.-Y. *J. Chem. Soc., Dalton Trans.* **1995**, 2323.
- (8) Whittaker, M. M.; Chuang, Y.-Y.; Whittaker, J. W. *J. Am. Chem. Soc.* **1993**, 115, 10029.
- (9) After the initial submission of this manuscript a few reports in the line of the present work have appeared. (a) Adams, H.; Bailey, N. A.; Campbell, I. K.; Fenton, D. E.; He, Q.-Y. *J. Chem. Soc., Dalton Trans.* **1996**, 2233. (b) Whittaker, J. W.; Duncan, W. R.; Whittaker, J. W. *Inorg. Chem.* **1996**, 35, 382. (c) Itoh, S.; Takayama, S.; Arakawa, R.; Furuta, A.; Komatsu, M.; Ishida, A.; Takamuku, S.; Fukuzumi, S. *Inorg. Chem.* **1997**, 36, 1407.
- (10) After the submission of the manuscript, the oxidation chemistry of several Cu(II) complexes with one or two phenolates has also been reported. Tolman et al. have studied synthetic models of the inactive copper(II) and tyrosinate and active copper(II)-tyrosyl radical forms of GOase and GIOase. (a) Halfen, J. A.; Young, V. G., Jr.; Tolman, W. B. *Angew. Chem.* **1996**, 35, 1687. (b) Halfen, J. A.; Jazdzewski, B. A.; Mahapatra, M.; Berreau, L. M.; Wilkinson, E. C.; Que, L., Jr.; Tolman, W. B. *J. Am. Chem. Soc.* **1997**, 119, 8217. Stack et al. have presented a family of functional models for GOase that catalytically oxidize benzylic and allylic alcohols to aldehydes with O_2 under mild conditions. (c) Wang, Y.; Stack, T. D. P. *J. Am. Chem. Soc.* **1996**, 118, 13097. (d) Wang, Y.; DuBois, J. L.; Hedman, B.; Hodgson, K.; Stack, T. D. P. *Science* **1998**, 279, 537. Pierre et al. have demonstrated that the phenoxyl radical-copper(II) nature of the one-electron oxidation product of a copper(II) complex with a N_2O_2 coordination sphere. (e) Zurita, D.; Gautier-Luneau, I.; Menage, S.; Pierre, J.-L.; Saint-Aman, E. *J. Biol. Inorg. Chem.* **1997**, 2, 46.
- (11) Whittaker, J. W. In *Metal Ions in Biological Systems*; Sigel, H., Ed.; Marcel Dekker, Inc.: Basel, Switzerland, 1994; pp 315-360.

- (12) Preliminary work presented at "ICBIC 7", Seventh International Conference on Bioinorganic Chemistry, September 3-8, 1995, Lübeck, Germany. Vaidyanathan, M.; Justin Thomas, K. R.; Palaniandavar, M. *J. Inorg. Biochem.* **1995**, 59, 686.
- (13) (a) *Organic Syntheses*; Horning, E. C., Ed.; John Wiley & Sons: New York, 1955; Vol. III, p 468. (b) Nishida, Y.; Shimo, H.; Kida, S. *J. Chem. Soc., Chem. Commun.* **1984**, 1611.

Table 1. Crystallographic Data for the Complexes

	1	2	3
chemical formula	C ₂₁ N ₇ H ₂₁ -CuO ₃ S ₂	C ₃₀ H ₃₄ -CuN ₄ O ₆	C ₁₉ H ₁₇ Cl-CuN ₄ O ₇
formula weight	547.11	610.17	512.36
crystal system	triclinic	triclinic	monoclinic
space group	<i>P</i> 1	<i>P</i> 1	<i>C</i> 2/ <i>c</i>
<i>a</i> , Å	10.796(2)	10.480(6)	13.417(3)
<i>b</i> , Å	10.804(2)	12.116(4)	20.095(2)
<i>c</i> , Å	12.559(2)	12.547(3)	16.401(2)
α , deg	71.38(1)	98.77(3)	
β , deg	72.68(1)	113.37(3)	102.21(2)
γ , deg	61.69(1)	100.78(3)	
<i>V</i> , Å ³	1203.2(3)	1390.5(10)	4321.8(10)
<i>Z</i>	2	2	8
<i>T</i> , K	298(2)	293(2)	296(2)
Mo K α radiation, λ , Å	0.710 73	0.710 73	0.710 73
ρ (calcd), g/cm ³	1.510	1.340	1.575
μ , mm ⁻¹	1.119	0.837	1.183
residuals [<i>I</i> > 2 σ (<i>I</i>)]			
<i>R</i> ^a	0.0296	0.0646	0.0449
<i>R</i> _w ^b	0.0669	0.1700	0.1108

$$^a R = \sum ||F_o| - |F_c|| / \sum |F_o|. \quad ^b R_w = [\sum w(F_o^2 - F_c^2)^2 / \sum w(F_o^2)^2]^{1/2}.$$

for data collection with an Enraf-Nonius CAD4 diffractometer employing Mo K α radiation. The reflections were centered and the cell parameters refined by least-squares method. The intensity of two reflections chosen were monitored at an interval of every 100 reflections. Over the entire period of data collection the variation of these intensities were very much below 10%. Finally, the intensity data sets were subjected to Lorentz polarization and absorption corrections using the MolEN¹⁴ program. The details regarding the data collection and processing are presented in Table 1.

From the systematic absences and *E* statistics of the data set the space group *C*2/*c* was assigned for **3**. For **1** and **2** there were no systematic absences in the data set and their structures were solved in the *P*1 space group, as the *E* statistics revealed a centric distribution. These space groups were later confirmed by the successful structure solution and refinement. All the structures were solved by heavy atom method using SHELXS 86 program¹⁵ and refined by full-matrix least-squares method on *F*² using SHELXS 93 program.¹⁶ For **3** all the non-hydrogen atoms except the nitro group were revealed by the first *E* map. The atoms of the nitro group were located during the first cycle of refinement. For **1**, all the non-hydrogen atoms except the ammonium nitrogen were found out by the first *E* map. The ammonium nitrogen was located by the subsequent Fourier map calculated after two cycles of isotropic refinement. For **1** and **3** all the hydrogens were located by difference Fourier synthesis; however, for **2** they were geometrically fixed using SHELXL 93 and assigned isotropic temperature factor of 0.15 Å² and included in the *R* value (0.0646) calculation. The non-hydrogen atoms were refined anisotropically and the hydrogens isotropically to final *R* values of 0.0296 and 0.0449 for **1** and **3**, respectively. The molecular structures were drawn using ORTEP-II.¹⁷ The final atomic coordinates are given in Tables 2a–c.

Results and Discussion

The tripodal ligand Hbnpn has been suggested⁶ to be a flexible ligand and form complexes with structures exhibiting a range of conformations. The para-substituted phenolic moiety in this ligand resembles the amino acid tyrosine,¹⁸ and the pyridine

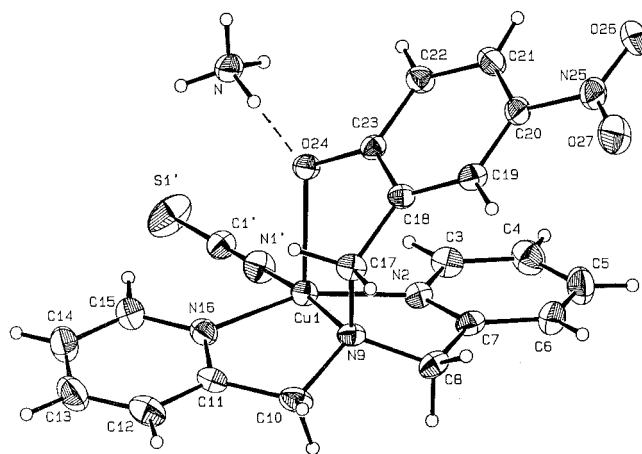


Figure 1. ORTEP drawing of [Cu(bnpn)(SCN)]·NH₄SCN showing the atom numbering scheme and the thermal motion ellipsoids (50% probability level) for the non-hydrogen atoms. Hydrogen atoms are omitted for clarity.

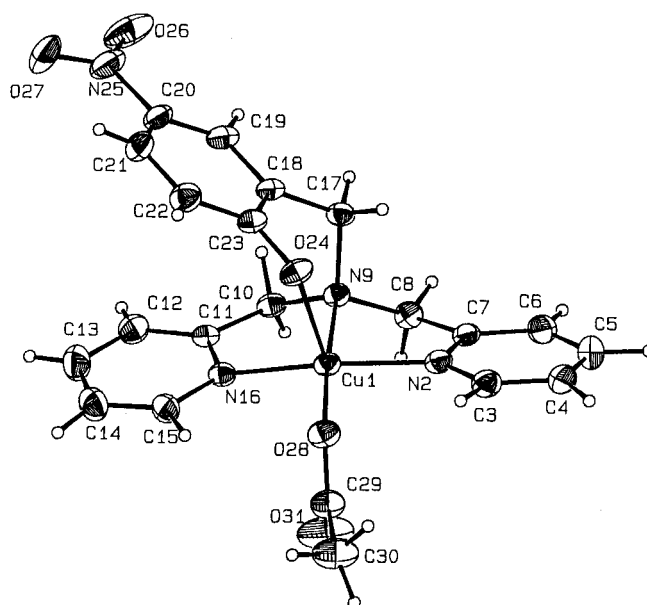


Figure 2. ORTEP drawing of [Cu(bnpn)(CH₃COO)]·CH₃OH·C₈H₁₀ showing the atom numbering scheme and the thermal motion ellipsoids (50% probability level) for the non-hydrogen atoms. Hydrogen atoms and the solvent molecules are omitted for clarity.

(py) nitrogens mimic the histidine imidazole in the active site of GOase. All the complexes are insoluble in water but are soluble in methanol, acetonitrile, and dimethylformamide; however, interestingly, the acetate complex **2** is soluble in water while the perchlorate **3** is insoluble in methanol.

Description of the Crystal Structures of [Cu(bnpn)(SCN)]·NH₄SCN (1**), [Cu(bnpn)(CH₃COO)]·CH₃OH·C₈H₁₀ (**2**),¹⁹ and [Cu(bnpn)ClO₄] (**3**).** The ORTEP plots of **1**, **2**, and **3** are depicted respectively in Figures 1, 2, and 3 with atom numbering scheme. The selected bond lengths and bond angles are given in Tables 3a–c. In the crystal structure of **1** the copper ion is coordinated to the two pyridine and tertiary amine nitrogens of the bnpn ligand and the SCN[−] nitrogen in the equatorial plane

(14) Rontgenweg, B. V. *MolEN Structure Determination System*; Delft Instruments, X-ray diffraction, 1: 2644 BD Delft, The Netherlands, 1990.

(15) Sheldrick, G. M. *SHELXS 86: Program for Automatic Structure Solution*; Göttingen, 1986.

(16) Sheldrick, G. M. *SHELXS 93*; University of Göttingen, 1993.

(17) Johnson, C. K. In *ORTEP II: A Program for Thermal Ellipsoidal Plotting*; Oak Ridge National Laboratory: Oak Ridge, TN, 1976.

(18) Van Landschoot, R. C.; Van Hest J. A. M.; Reedijk, J. *Inorg. Chim. Acta* **1983**, 72, 89.

(19) After the submission of this manuscript Fenton et al. have reported the complex [Cu(bnpn)(acetate)]·H₂O whose structure is essentially the same as the present one but with $\tau = 0.17$. No EPR or electrochemical data were provided to allow comparisons with the present compounds.^{9a}

Table 2. Atomic Coordinates ($\times 10^4$) and Equivalent Isotropic Displacement Coefficients ($\text{\AA}^2 \times 10^3$)

atom	x	y	z	$U(\text{eq})^a$	atom	x	y	z	$U(\text{eq})^a$
(a) For $[\text{Cu}(\text{bnpn})(\text{SCN})]\cdot\text{NH}_4\text{SCN}$ (1)									
Cu(1)	754(1)	-99(1)	3052(1)	32(1)	C(18)	-1192(2)	236(2)	1335(2)	31(1)
N(2)	-1251(2)	881(2)	3813(2)	35(1)	C(19)	-2490(3)	483(3)	1137(2)	36(1)
C(3)	-1849(3)	2197(3)	4055(2)	44(1)	C(20)	-3447(2)	1872(3)	762(2)	38(1)
C(4)	-3284(3)	2870(3)	4450(2)	54(1)	C(21)	-3124(3)	3035(3)	552(2)	42(1)
C(5)	-4136(3)	2202(4)	4576(3)	60(1)	C(22)	-1829(3)	2804(3)	729(2)	39(1)
C(6)	-3542(3)	874(3)	4312(2)	51(1)	C(23)	-826(2)	1406(2)	1133(2)	31(1)
C(7)	-2088(3)	224(3)	3947(2)	37(1)	O(24)	390(2)	1164(2)	1336(1)	36(1)
C(8)	-1332(3)	-1280(3)	3746(2)	41(1)	N(25)	-4832(2)	2132(3)	605(2)	48(1)
N(9)	47(2)	-1505(2)	2955(2)	32(1)	O(26)	-5713(2)	3389(2)	351(2)	62(1)
C(10)	1188(3)	-2975(3)	3255(3)	45(1)	O(27)	-5104(2)	1108(2)	742(2)	67(1)
C(11)	2627(3)	-2951(2)	2825(2)	41(1)	N(1')	1479(2)	1095(2)	3325(2)	47(1)
C(12)	3876(4)	-4155(3)	2608(3)	58(1)	C(1')	2096(3)	1733(3)	3300(2)	39(1)
C(13)	5157(3)	-4051(3)	2295(3)	64(1)	S(1')	2945(1)	2619(1)	3292(1)	79(1)
C(14)	5178(3)	-2756(4)	2173(3)	59(1)	S(2')	-1790(1)	-4406(1)	3964(1)	65(1)
C(15)	3914(3)	-1588(3)	2377(2)	49(1)	C(2')	-1294(3)	-4484(3)	2628(3)	48(1)
N(16)	2655(2)	-1689(2)	2711(2)	40(1)	N(2')	-946(3)	-4521(3)	1672(2)	71(1)
C(17)	-124(3)	-1245(2)	1748(2)	35(1)	N'	1503(2)	3125(3)	645(2)	47(1)
(b) For $[\text{Cu}(\text{bnpn})(\text{CH}_3\text{COO})]\cdot\text{CH}_3\text{OH}\cdot\text{C}_8\text{H}_{10}$ (2)									
Cu	1787(1)	3246(1)	2226(1)	36(1)	C22	-1338(6)	1807(5)	-1277(5)	53(1)
N2	3386(4)	2614(3)	3170(3)	40(1)	C23	-386(5)	1703(4)	-157(4)	40(1)
C3	4707(6)	2811(5)	3227(5)	49(1)	O24	989(3)	2262(3)	357(3)	46(1)
C4	5724(6)	2328(5)	3906(5)	55(1)	N25	-4849(6)	-35(6)	-1713(6)	77(2)
C5	-5388(7)	-1627(6)	-4579(6)	62(2)	O26	-5284(5)	-758(6)	-1259(5)	100(2)
C6	4021(6)	1409(5)	4518(5)	53(1)	O27	-5647(5)	228(5)	-2617(5)	109(2)
C7	3045(5)	1918(4)	3810(4)	39(1)	O28	3049(4)	4467(3)	1993(3)	47(1)
C8	1561(5)	1790(4)	3750(4)	43(1)	C29	3689(6)	5418(5)	2793(5)	50(1)
N9	564(4)	1968(3)	2598(3)	34(1)	C30	4797(8)	6249(6)	2601(7)	77(2)
C10	-679(5)	2334(4)	2668(4)	39(1)	O31	3473(6)	5682(5)	3662(5)	96(2)
C11	-1030(5)	3234(4)	1980(4)	37(1)	O32	2147(5)	2124(5)	8866(4)	39(1)
C12	-2364(6)	3454(5)	1578(5)	56(1)	C33	3604(9)	2632(8)	9463(8)	87(2)
C13	-2574(6)	4344(6)	1020(6)	68(2)	C34	1302(7)	4855(5)	5006(5)	63(2)
C14	-1453(7)	5003(5)	890(6)	60(2)	C35	631(7)	5600(5)	4410(5)	61(2)
C15	-161(6)	4736(4)	1293(5)	47(1)	C36	649(7)	4262(5)	5618(5)	61(2)
N16	63(4)	3860(3)	1828(3)	37(1)	C37	-9837(5)	1885(4)	-3368(4)	39(1)
C17	39(5)	872(4)	1629(4)	41(1)	C38	-9886(6)	957(5)	-4157(5)	49(1)
C18	-956(5)	981(4)	434(4)	38(1)	C39	-11087(5)	549(5)	-5278(5)	49(1)
C19	-2419(5)	404(4)	-100(5)	46(1)	C40	-8808(5)	388(5)	-3901(5)	49(1)
C20	-3310(5)	542(5)	-1186(5)	51(1)	C41	2520(6)	4646(5)	5020(5)	51(1)
C21	-2780(6)	1233(5)	-1781(5)	60(2)					
(c) For $[\text{Cu}(\text{bnpn})\text{ClO}_4]$ (3)									
Cu(1)	2207(1)	3252(1)	5061(1)	40(1)	C(17)	2371(4)	3454(2)	6851(2)	43(1)
N(2)	3543(3)	3750(2)	5395(2)	48(1)	C(18)	2001(3)	2772(2)	6991(2)	40(1)
C(3)	4474(4)	3602(3)	5286(3)	60(1)	C(19)	1590(3)	2653(2)	7687(2)	46(1)
C(4)	5312(5)	3980(4)	5600(4)	87(2)	C(20)	1340(3)	2016(2)	7872(2)	47(1)
C(5)	5188(7)	4539(4)	6047(5)	104(3)	C(21)	1499(4)	1479(2)	7388(3)	48(1)
C(6)	4240(6)	4698(3)	6176(4)	81(2)	C(22)	1898(4)	1590(2)	6690(3)	48(1)
C(7)	3430(4)	4297(2)	5843(3)	55(1)	C(23)	2139(3)	2232(2)	6470(2)	37(1)
C(8)	2352(5)	4416(2)	5948(3)	59(1)	O(24)	2512(2)	2346(1)	5798(2)	42(1)
N(9)	1876(3)	3757(2)	6031(2)	43(1)	N(25)	934(3)	1897(2)	8614(2)	62(1)
C(10)	761(4)	3824(3)	5950(3)	57(1)	O(26)	689(3)	2370(2)	8991(2)	82(1)
C(11)	212(3)	3705(2)	5069(3)	48(1)	O(27)	849(4)	1324(2)	8830(2)	89(1)
C(12)	-772(4)	3915(3)	4779(4)	75(2)	Cl(28)	1764(1)	5122(1)	3452(1)	66(1)
C(13)	-1251(5)	3779(4)	3976(5)	99(2)	O(29)	2256(5)	4933(2)	2821(3)	140(2)
C(14)	-720(6)	3428(4)	3479(5)	110(3)	O(30)	1343(6)	5719(3)	3300(4)	188(4)
C(15)	249(5)	3231(3)	3801(4)	79(2)	O(31)	1131(7)	4689(4)	3704(5)	214(4)
N(16)	724(3)	3369(2)	4581(2)	50(1)	O(32)	2475(5)	5135(6)	4180(4)	244(6)

^a U_{eq} is defined as one-third of the trace of the orthogonalized U_{ij} tensor.

and to the phenolate oxygen of the bnpn ligand in the axial position. The coordination structure is similar to that of its chloride analogue,⁶ and thus the geometry around copper(II) is best described as square pyramidal with a small trigonal component as revealed by the trigonal index²⁰ τ of 0.24 [$\tau = (\beta - \alpha)/60$, where $\alpha = \text{N}'\text{-Cu-N9} = 173.1(1)^\circ$ and $\beta = \text{N2-Cu-N16} = 158.7(1)^\circ$; for perfect square pyramidal and trigonal bipyramidal geometries, the τ values are zero and unity

respectively]. Copper is displaced 0.208 Å above the CuN₄ coordination plane and toward the axially coordinated phenolate oxygen. The coordinated SCN⁻ ion is nearly linear with the N4-C22-S bond angle of 178°. It is interesting to note that the axial phenolate oxygen is hydrogen-bonded to NH₄⁺ ion which in turn is hydrogen-bonded to the nitrogen atom of uncoordinated NCS⁻ ion.

In the crystal structure of **2** the copper ion is coordinated to the two pyridine and tertiary amine nitrogens of the bnpn ligand and the acetate oxygen in the equatorial plane and to the phenolate oxygen of the bnpn ligand in the axial position. The

(20) Addison, A. W.; Rao, T. N.; Reedijk, J.; Van Rijn, J.; Verschoor, G. *J. Chem. Soc., Dalton Trans.* **1984**, 1349.

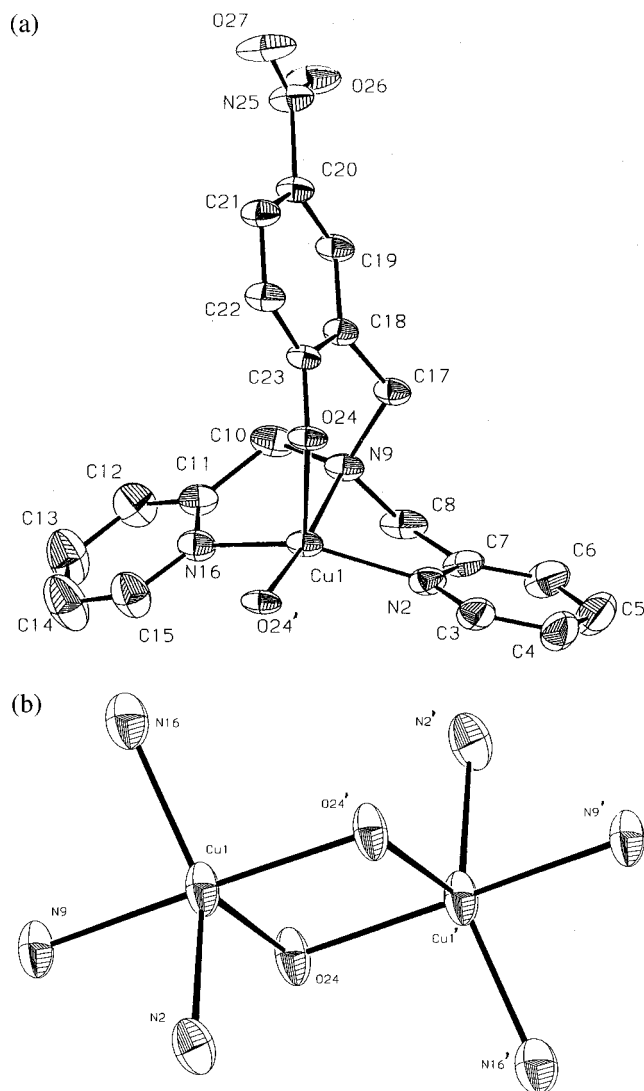


Figure 3. (a) ORTEP drawing of $[\text{Cu}(\text{bnp})(\text{ClO}_4)]$ showing the atom numbering scheme and the thermal motion ellipsoids (50% probability level) for the non-hydrogen atoms. Hydrogen atoms are omitted for clarity. (b) Coordination core structure of **3**.

coordination structure is similar to that of its chloride⁶ and thiocyanate analogues. The geometry around copper(II) is best described as square pyramidal with a small trigonal component²⁰ ($\tau = 0.29$). Copper is displaced 0.167 Å above the CuN_3O coordination plane and toward the axially coordinated phenolate oxygen.

The complex cation of **3** is a centrosymmetric dimer composed of two distorted square-based $\text{Cu}(\text{II})$ coordination spheres. Each copper(II) ion is coordinated to a tertiary amine and two pyridine nitrogens of the bnp ligand and a phenolate from the second coordination sphere, in the basal plane and the square-based geometry completed by the axial coordination of the first phenolate to form an unsymmetrically bridged Cu_2O_2 core. The two parts of the dimer are trans to each other and the $\text{Cu}\cdots\text{Cu}$ distance is 3.09 Å. The trigonality index ($\tau = 0.48$) for the perchlorate is higher than those for the Cl^- , SCN^- , and CH_3COO^- complexes, suggesting an increase in trigonality and hence steric constraints at the copper on dimerization. Thus copper is displaced 0.143 Å away from the CuN_3O coordination plane but opposite to the axial $\text{Cu}(\text{II})$ –phenolate bond, unlike in the other three complexes (Table 4).

The present structure is different from the above monomeric $[\text{Cu}(\text{L})\text{X}]$ [$\text{X}^- = \text{Cl}^-$, SCN^- , CH_3COO^-] complexes in that it

Table 3. Selected Bond Distances (Å) and Angles (deg)

(a) For $[\text{Cu}(\text{bnp})(\text{SCN})]\cdot\text{NH}_4\text{SCN}$ (1)			
$\text{Cu}(1)-\text{N}1'$	1.947(2)	$\text{Cu}(1)-\text{N}(16)$	1.987(2)
$\text{Cu}(1)-\text{N}(9)$	2.044(2)	$\text{Cu}(1)-\text{N}(2)$	1.990(2)
$\text{Cu}(1)-\text{O}(24)$	2.186(2)	$\text{N}(2)-\text{C}(3)$	1.348(4)
$\text{N}(2)-\text{C}(7)$	1.338(4)	$\text{N}(9)-\text{C}(10)$	1.490(3)
$\text{N}(9)-\text{C}(17)$	1.503(3)	$\text{C}(11)-\text{N}(16)$	1.339(3)
$\text{N}1'-\text{Cu}(1)-\text{N}(16)$	95.8(1)	$\text{N}1'-\text{Cu}(1)-\text{N}(2)$	96.2(1)
$\text{N}1'-\text{Cu}(1)-\text{N}(9)$	173.1(1)	$\text{N}1'-\text{Cu}(1)-\text{O}(24)$	94.1(1)
$\text{N}(16)-\text{Cu}(1)-\text{N}(9)$	82.4(1)	$\text{N}(16)-\text{Cu}(1)-\text{N}(2)$	158.7(1)
$\text{N}(9)-\text{Cu}(1)-\text{N}(2)$	83.5(1)	$\text{N}(16)-\text{Cu}(1)-\text{O}(24)$	101.3(1)
$\text{N}(9)-\text{Cu}(1)-\text{O}(24)$	92.9(1)	$\text{N}(2)-\text{Cu}(1)-\text{O}(24)$	95.2(1)
(b) For $[\text{Cu}(\text{bnp})(\text{CH}_3\text{COO})]\cdot\text{CH}_3\text{OH}\cdot\text{C}_8\text{H}_{10}$ (2)			
$\text{Cu}-\text{N}2$	1.995(4)	$\text{Cu}-\text{N}9$	2.052(4)
$\text{Cu}-\text{N}16$	1.992(4)	$\text{Cu}-\text{O}24$	2.200(3)
$\text{C}15-\text{N}16$	1.349(6)	$\text{Cu}-\text{O}28$	1.931(3)
$\text{N}2-\text{C}3$	1.331(6)	$\text{N}2-\text{C}7$	1.344(6)
$\text{N}9-\text{C}10$	1.482(6)	$\text{N}9-\text{C}17$	1.500(6)
$\text{C}11-\text{N}16$	1.347(6)	$\text{C}23-\text{O}24$	1.310(6)
$\text{N}25-\text{O}27$	1.243(8)	$\text{O}28-\text{C}29$	1.269(6)
$\text{C}29-\text{C}30$	1.510(7)	$\text{C}29-\text{O}31$	1.208(7)
$\text{O}24-\text{Cu}-\text{O}28$	90.66(14)	$\text{N}16-\text{Cu}-\text{O}28$	99.4(2)
$\text{N}16-\text{Cu}-\text{O}24$	92.1(2)	$\text{N}9-\text{Cu}-\text{O}28$	175.77(14)
$\text{N}9-\text{Cu}-\text{O}24$	92.70(14)	$\text{N}9-\text{Cu}-\text{N}16$	83.0(2)
$\text{N}2-\text{Cu}-\text{O}28$	93.9(2)	$\text{N}2-\text{Cu}-\text{O}24$	104.8(2)
$\text{N}2-\text{Cu}-\text{N}16$	158.4(2)	$\text{N}2-\text{Cu}-\text{N}9$	82.7(2)
$\text{Cu}-\text{N}2-\text{C}7$	114.0(4)	$\text{Cu}-\text{N}2-\text{C}3$	127.4(4)
$\text{C}3-\text{N}2-\text{C}7$	118.5(5)	$\text{N}2-\text{C}3-\text{C}4$	122.5(6)
$\text{N}2-\text{C}7-\text{C}6$	121.9(6)	$\text{C}6-\text{C}7-\text{C}8$	122.7(5)
$\text{N}2-\text{C}7-\text{C}8$	115.3(5)	$\text{C}7-\text{C}8-\text{N}9$	110.4(5)
$\text{Cu}-\text{N}9-\text{C}8$	105.6(3)	$\text{C}8-\text{N}9-\text{C}17$	109.3(4)
$\text{C}8-\text{N}9-\text{C}10$	112.8(4)	$\text{Cu}-\text{N}9-\text{C}17$	109.1(3)
$\text{Cu}-\text{N}9-\text{C}10$	109.8(3)	$\text{C}10-\text{N}9-\text{C}17$	110.1(4)
$\text{N}9-\text{C}10-\text{C}11$	110.9(5)	$\text{C}10-\text{C}11-\text{N}16$	115.9(5)
$\text{C}11-\text{N}16-\text{C}15$	118.5(5)	$\text{Cu}-\text{N}16-\text{C}15$	125.8(4)
$\text{Cu}-\text{N}16-\text{C}11$	115.2(4)	$\text{Cu}-\text{O}24-\text{C}23$	114.2(3)
$\text{C}20-\text{N}25-\text{O}27$	117.3(6)	$\text{C}20-\text{N}25-\text{O}26$	118.9(6)
$\text{O}26-\text{N}25-\text{O}27$	123.8(7)	$\text{Cu}-\text{O}28-\text{C}29$	119.5(4)
(c) For $[\text{Cu}(\text{bnp})(\text{ClO}_4)]$ (3)			
$\text{Cu}(1)-\text{O}24'$	1.947(2)	$\text{Cu}(1)-\text{N}(16)$	1.993(4)
$\text{Cu}(1)-\text{N}(9)$	2.014(3)	$\text{Cu}(1)-\text{N}(2)$	2.025(4)
$\text{Cu}(1)-\text{O}(24)$	2.174(3)	$\text{N}(2)-\text{C}(3)$	1.333(6)
$\text{N}(2)-\text{C}(7)$	1.348(5)	$\text{N}(9)-\text{C}(10)$	1.480(6)
$\text{N}(9)-\text{C}(17)$	1.498(5)	$\text{C}(11)-\text{N}(16)$	1.342(5)
$\text{O}(24')-\text{Cu}(1)-\text{N}(16)$	96.69(13)	$\text{O}(24')-\text{Cu}(1)-\text{N}(2)$	101.86(12)
$\text{O}(24')-\text{Cu}(1)-\text{N}(9)$	172.19(12)	$\text{O}(24')-\text{Cu}(1)-\text{O}(24)$	80.97(10)
$\text{N}(16)-\text{Cu}(1)-\text{N}(9)$	83.35(14)	$\text{N}(16)-\text{Cu}(1)-\text{N}(2)$	143.2(2)
$\text{N}(9)-\text{Cu}(1)-\text{N}(2)$	82.37(14)	$\text{N}(16)-\text{Cu}(1)-\text{O}(24)$	111.95(13)
$\text{N}(9)-\text{Cu}(1)-\text{O}(24)$	91.75(11)	$\text{N}(2)-\text{Cu}(1)-\text{O}(24)$	102.25(13)
$\text{C}(3)-\text{N}(2)-\text{Cu}(1)$	130.9(3)	$\text{C}(7)-\text{N}(2)-\text{Cu}(1)$	110.9(3)
$\text{C}(10)-\text{N}(9)-\text{Cu}(1)$	111.3(3)	$\text{C}(8)-\text{N}(9)-\text{Cu}(1)$	101.9(2)
$\text{C}(17)-\text{N}(9)-\text{Cu}(1)$	112.0(2)	$\text{C}(15)-\text{N}(16)-\text{Cu}(1)$	126.2(3)
$\text{C}(11)-\text{N}(16)-\text{Cu}(1)$	114.7(3)	$\text{C}(23)-\text{O}(24)-\text{Cu}(1)$	123.2(2)
$\text{C}(23)-\text{O}(24)-\text{Cu}(1)'$	131.3(2)	$\text{Cu}(1)'\text{-O}(24)-\text{Cu}(1)$	99.03(10)

is dimeric, but is similar to them in that the $\text{Cu}(\text{II})$ –phenolate bond is axial. The dimerization appears to be due to the inability of the perchlorate ion to coordinate strongly in the equatorial position, which leads to the coordinated phenolate group in the neighboring molecule to default²¹ to the equatorial position in the first molecule.

Comparison of Structures and Significance of Axial Phenolate Coordination. All the present complexes are best described as having trigonal bipyramidal distorted square based pyramidal stereochemistry (TBDSBP).²² For **1** and **2** the observed displacement of the metal out of the basal plane toward

(21) (a) Addison, A. W.; Burke, P. J.; Henrick, K.; Nageswara Rao, T.; Sinn, E. *Inorg. Chem.* **1983**, 22, 3645. (b) Palaniandavar, M.; Pandiyan, T.; Lakshminarayanan, M.; Manohar, H. *J. Chem. Soc., Dalton Trans.* **1995**, 455.

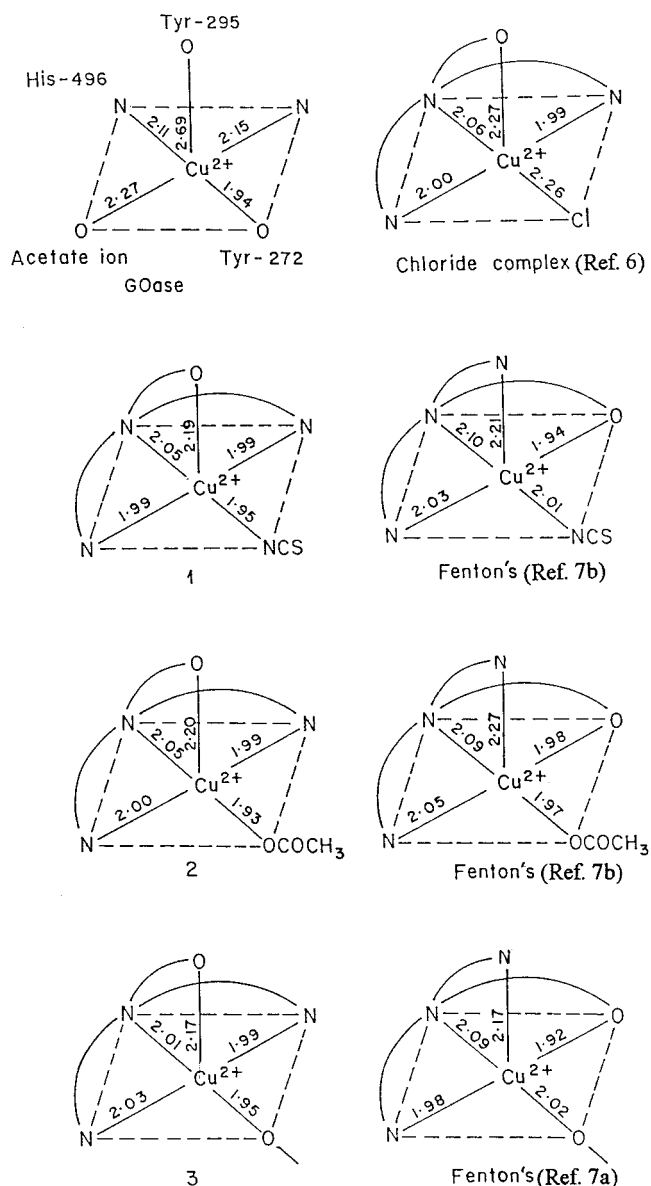
Table 4. Comparison of Selected Bond Lengths (Å) and Bond Angles (deg) of Model Complexes

	Cu(bppn)Cl	NCS ⁻		CH ₃ COO ⁻		ClO ₄ ⁻	
		1	Fenton's	2	Fenton's	3	Fenton's
Cu—N(py)	1.986(1)	1.990(2)	2.026(5)	1.995(4)	2.046(3)	2.025(4)	1.983(15)
Cu—N(py)	1.997(1)	1.987(2)	2.205(5)	1.992(4)	2.265(3)	1.993(4)	2.168(13)
Cu—N(imine)	2.060(1)	2.044(2)	2.100(4)	2.052(4)	2.085(3)	2.014(3)	2.085(13)
Cu—O(axial/equatorial phenolate)	2.268(2)	2.186(2)	1.938(4)	2.200(3)	1.982(3)	2.174(3)	1.922(12)
Cu—Cl/N'(NCS)/O(acetate)/O(phenolate)	2.256(1)	1.947(2)	2.012(6)	1.931(3)	1.970(2)	1.947(2)	2.019(12)
deviation of Cu from equatorial plane	-0.2258	+0.2081	-0.259	+0.1628	+0.161	-0.1433	+0.252
N(py)—Cu—N(py)	160.1(1)	158.75(8)	161.1(2)	158.4(2)	171.9(1)	143.2(2)	167.5(6)
N(imine)—Cu—Cl/N'(NCS)/O(acetate)/O(phenolate)	169.6(1)	173.04(8)	167.9(2)	175.77(14)	167.4(1)	172.19(12)	157.6(5)
τ	0.16	0.24	0.11	0.28	0.076	0.48	0.17
ref	6	this work	7b	this work	7b	this work	7a

the axial ligand in otherwise square pyramidal geometry appears to be the rule rather than the exception.²³ The axial Cu(II)—phenolate bonds in the present mono- and binuclear complexes are unusual. This is in remarkable contrast to the equatorial Cu(II)—phenolate bond observed in the analogous complex [Cu(L)N₃] [HL = *N,N*-bis(pyrid-2-ylethyl)-2-methylaminophenol]²⁴ and in the homologues [Cu(L)X] [HL = 2-[bis(pyrid-2-ylethyl)aminomethyl]-4-nitrophenol, X⁻ = SCN⁻, CH₃COO⁻]⁷ (Figure 4), all of which contain a 6,6,6-membered chelate ring sequence at the copper atom whereas the present complexes possess a 5,5,6-chelate ring sequence. So it is suggested that the nature of chelate rings formed and the consequent steric factors involved are responsible for the axial coordination of *p*-nitrophenolate ion in the present complexes; the steric constraint at copper increases on replacing the six-membered chelate rings by five-membered ones. Thus the τ values (SCN⁻, 0.11; CH₃COO⁻, 0.08; and ClO₄⁻, 0.17) for the homologues are lower than those for the corresponding complexes in the present series (0.16–0.48, Table 4). Further, the stronger coordination of the five-membered chelate rings in the equatorial plane of the present compounds is implied by the equatorial Cu—N_{py} bonds [1.986(2)–2.025(5) Å] which are shorter than those of the respective homologues [SCN⁻, 2.026(5); CH₃COO⁻, 2.046(3); and ClO₄⁻, 1.983(15) Å]. Thus in the present compounds the extension of one of the tripodal arms (six-membered ring) and hence its large flexibility²⁵ favors the stronger phenolate donor to occupy the axial position (against Jahn–Teller distortion) and in the homologues the stronger phenolate donor defaults to the equatorial position, as expected.²¹

As a consequence of the axial phenolate coordination both the pyridine nitrogen donors in the present complexes occupy trans-equatorial sites, whereas one of the pyridines in the homologues⁷ and in the azide²⁴ complex takes up the axial position. Thus the N_{py}—Cu—N_{py} bond angle changes from 99.8 to 158.7° in the thiocyanates, from 95.7 to 158.4° in the acetates and from 98.1 to 143.2° in the perchlorates. However, this angle is less than that (168–178°) for other Cu(II) complexes containing two coordinating pyridine moieties and adopting a square pyramidal geometry²⁶ in a binuclear environment.

The dimeric structure of **3** is similar to that of the unsubstituted homologous perchlorate complex [Cu(L)ClO₄] [HL = 2-[bis(pyrid-2-ylethyl)aminomethyl]phenol]^{7a,27} and the related

**Figure 4.** Comparison of copper(II) coordination environments.

complex reported²⁶ by Karlin et al. However, the phenolates in the latter two complexes are coordinated cis-equatorially while contrastingly they are coordinated in a cis-axial/equatorial fashion in **3**. The bond between the two parts of the dimer in

- (22) Murphy, G.; Nagle, P.; Murphy, B.; Hathaway, B. *J. Chem. Soc., Dalton Trans.* **1997**, 2645.
 (23) (a) Hoskins, B. F.; Whillans, F. D. *Coord. Chem. Rev.* **1972**, 9, 365.
 (b) Addison, A. W.; Carpenter, M.; Lau, L. K.-M.; Wicholas, M. *Inorg. Chem.* **1978**, 17, 1545.
 (24) Karlin, K. D.; Cohen, B. I.; Hayes, J. C.; Farooq, A.; Zubieta, J. *Inorg. Chem.* **1987**, 26, 147.
 (25) Alilou, E. I.; Amadei, E.; Giorgi, M.; Pierrot, M.; Reglier, M. *J. Chem. Soc., Dalton Trans.* **1993**, 549.
 (26) Karlin, K. D.; Hayes, J. C.; Gultneih, Y.; Cruse, R. W.; McKown, J. W.; Hutchinson, J. P.; Zubieta, J. *J. Am. Chem. Soc.* **1984**, 106, 2121.

- (27) After the submission of this manuscript Fenton et al. reported a complex but without a *p*-NO₂ substituted unsubstituted complex analogous to **3**. The less accurate coordination structure is essentially the same as the present one, but τ = 0.31; Cu—O(axial), 2.177(9) Å; Cu—Cu, 3.153 Å. No EPR or electrochemical data were reported.^{9a}

Table 5. Spectral and Redox Properties of [Cu(bnp)X] Complexes

complex	electronic spectra $\bar{\nu}_{\max} \times 10^3 \text{ cm}^{-1}(\epsilon, \text{M}^{-1} \text{cm}^{-1})$		EPR spectra ^b		redox ^g			
	solid	solution	solid	frozen solution	solvent/supporting electrolyte	$E_{1/2}$ (V)	ΔE_p (mV)	D ($10^{-6} \text{ cm}^2 \text{ s}^{-1}$)
1	13.7	DMF	$g_{\parallel} 2.269$ $g_{\perp} 2.073$	MeOH	MeOH/ NEt_4BF_4	−0.53	210	7.9
		14.0 (240) 10.2 (160) 24.6 (36200) 20.6 (345) sh		$g_{\parallel} 2.217$ $A_{\parallel} 173$				
	14.9	ACN	$g_1 2.149$ $g_2 2.073$ $g_3 2.003$	ACN	MeCN/THAP ^d	−0.77	364	7.2
		13.9 (97) 25.1 (18570)		$g_{\parallel} 2.218$ $A_{\parallel} 174$				
2	15.3	MeOH	$g_o = 2.074$	MeOH	DMF/THAP	−0.85	120	2.8
		15.0 (225) 26.1 (26100)		$g_{\parallel} 2.225$ $A_{\parallel} 185$				
	15.7	ACN	$g_1 2.229^e$ $g_2 2.141$ $g_3 2.048$	DMF	MeCN/THAP	−0.64	108	16.2
		11.6 (136) 14.0 (121) 25.5 (20210)		$g_{\parallel} 2.228$ $A_{\parallel} 177$				
3	12.5	H ₂ O	$g_1 2.229^e$ $g_2 2.141$ $g_3 2.048$	DMF	MeCN/THAP	−0.64	108	16.2
		15.1 (135) 25.5 (20440)		$g_{\parallel} 2.242$ $A_{\parallel} 183$				
	12.5	ACN	$g_1 2.229^e$ $g_2 2.141$ $g_3 2.048$	DMF	MeCN/THAP	−0.64	108	16.2
		14.5 (112) 25.2 (23310)		$g_{\parallel} 2.228$ $A_{\parallel} 177$				
3	12.5	DMF ^e	$g_1 2.229^e$ $g_2 2.141$ $g_3 2.048$	DMF	MeCN/THAP	−0.64	108	16.2
		13.5 (140) 11.8 (150) 25.6 (16400)		$g_{\parallel} 2.276$ $A_{\parallel} 185$				
	12.5	ACN ^e	$g_1 2.229^e$ $g_2 2.141$ $g_3 2.048$	DMF	MeCN/THAP	−0.64	108	16.2
		12.5 (160) 28.5 (15370)		$g_{\parallel} 2.276$ $A_{\parallel} 185$				

^a Data taken from ref 6. ^b A_{\parallel} in 10^{-4} cm^{-1} . ^c Half-field signal ($\Delta M_s = \pm 2$) at 1650 gauss. ^d The complex was washed with water and used for electrochemistry. ^e Concentration based on monomer. ^f Five N-superhyperfine lines observed. ^g Scan rate: 50 mV/s.

3 ($\text{Cu} \cdots \text{Cu}$, 3.09 Å) appears to be slightly stronger than that in its homologue ($\text{Cu} \cdots \text{Cu}$, 3.13 Å) and as a consequence the Cu(II)–phenolate bonds in **3** become weaker than those in its homologue [Cu–O, 1.922(12), 2.019(12) Å]. It is interesting to note that the axial Cu(II)–phenolate bond (Cu–O, 2.174 Å) is longer than the equatorial one (1.947 Å). The axial Cu(II)–phenolate bond length varies dramatically with the change in equatorially sited anions in the order, $\text{Cl}^- > \text{CH}_3\text{COO}^- > \text{SCN}^- > \text{PhO}^- (\text{ClO}_4^-)$, showing the stronger coordination of chloride ion to Cu(II). The same order is exhibited by the Cu(II)– N_{py} axial bond lengths for the homologous compounds.⁷ These observations represent a clear manifestation of the Jahn–Teller effect in the copper(II) square pyramidal geometry.

Spectral Properties. The spectral behaviors of [Cu(bnp)X] complexes ($\text{X}^- = \text{Cl}^-, \text{SCN}^-, \text{CH}_3\text{COO}^-$, and ClO_4^-) are found to be anion and solvent dependent (Table 5). Thus the reflectance and solution spectral properties of the monomeric complexes are similar to each other, but are significantly different from those of the dimeric complex **3**, which is expected^{28,29} of the difference in their coordination geometries. The polycrystalline complex **3** exhibits two ligand field (LF) bands and a rhombic EPR spectrum, which are consistent with its trigonally distorted Cu(II) geometry; the $\Delta M_s = \pm 2$ signal around 1650 G in the EPR spectrum is typical of its dimeric structure. In contrast to **3**, the polycrystalline monomeric complexes exhibit only one visible band in the reflectance

spectra and rhombic, isotropic, or axial EPR spectrum. The relatively low values of $\bar{\nu}_{\max}$ (12 500–14 900 cm^{-1}) observed in the reflectance spectra of all these complexes are consistent with the observed displacement^{23b} of Cu(II) from the N_4 plane toward the axial phenolate, anion³⁰ or oxygen³¹ coordination and presence of trigonal element³² in the coordination geometries.

All the monomeric complexes exhibit only one LF band in MeOH solution. However, in acetonitrile solution the thiocyanate complex displays two ligand field bands. The unique behavior of thiocyanate is relevant to that of GOase enzyme^{5d} on adding SCN^- . In contrast, the homologous^{7b} thiocyanate and other monomeric complexes with equatorial phenolates display only one LF band. This suggests that the axial rather than the cis-equatorial phenolate enables SCN^- to coordinate strongly. The $\bar{\nu}_{\max}$ values (12 500–14 500 cm^{-1}) of the present complexes in solution are in general lower than those respectively of the homologues^{7b} (13 150–15 030 cm^{-1}) discussed above; this is expected of the stronger equatorial phenolate coordination and lower trigonal distortions observed in the homologues.^{7b} The cryogenic solution EPR spectra of all the complexes including **3** are axial,³³ suggesting the presence of a

(28) Harrison, D.; Kennedy, D.; Hathaway, B. J. *Inorg. Nucl. Chem. Lett.* **1981**, 170, 87.

(29) Tyagi, S.; Hathaway, B. J. *J. Chem. Soc., Dalton Trans.* **1981**, 2029.

(30) Hathaway, B. J. In *Comprehensive Coordination Chemistry*; Wilkinson, G., Gillard, R. G., McCleverty, J. A., Eds.; Pergamon Press: Oxford, 1987; Vol. 2, p 533.

(31) (a) West, D. X.; Palaniandavar, M. *Inorg. Chim. Acta* **1983**, 71, 61.

(b) West, D. X.; Palaniandavar, M. *Inorg. Chim. Acta* **1983**, 76, L149.

(c) West, D. X.; Palaniandavar, M. *Inorg. Chim. Acta* **1983**, 77, L97.

(32) Thompson, L. K.; Ramaswamy, B. S.; Dawe, R. D. *Can. J. Chem.* **1978**, 56, 1311.

Table 6. Electronic and EPR Spectral Effects of Anion Addition to GOase^{5d} and Cu(II) Complexes

enzyme/complex	anion added (ratio) ^c	electronic spectra ^a		EPR spectra ^b	
		ligand field λ_{\max} (ϵ_{\max})	charge transfer λ_{\max} (ϵ_{\max})	g_{\parallel}	A_{\parallel}
GOase	none	629	450	2.277	175
	CN ⁻ (1:10)	570	390	2.226	156
	N ₃ ⁻ (1:10)	570	390	2.253	171
2^d	none	662 (135)	392 (20 440)	2.243	180
	CN ⁻ (excess)	583 (65)	409 (17 140)	2.202	184
	N ₃ ⁻ (excess)	631 (354)	397 (24 170)	2.231	172
[Cu(cyclops)] ⁺ ^e	none	516 (150)		2.181	183
[Cu(cyclops)(CN)] ^e	none	730		2.187	169
[Cu(bnpn)Cl] ^f	none	721 (97)	398 (18 570)	—	—
	CN ⁻ (excess)	756 (110)	419 (38 600)	—	—
	N ₃ ⁻ (excess)	838 (160)	400 (27 390)	—	—
		695 (200)			

^a λ_{\max} in nm (ϵ_{\max} , M⁻¹ cm⁻¹). ^b A_{\parallel} in gauss. ^c Molar ratio (GOase/Cu:ligand). ^d In aqueous solution. ^e Reference 23b. ^f In acetonitrile solution.

$d_{x^2-y^2}$ ground state in Cu(II) located in square-based geometries. The $\Delta M_s = \pm 2$ signal of **3** observed in the solid state is not discernible in solution suggesting the partial dissociation of the dimeric complex to yield solvated monomeric species. The g_{\parallel} values lie in the range 2.22–2.28, suggesting the presence of a CuN₂O₂ or CuN₃O chromophore³⁴ in solution also, with the dimeric complex **3** having the highest g_{\parallel} [Cl⁻ < NCS⁻ < CH₃COO⁻ < ClO₄⁻ (CH₃CN)] and lowest $\bar{\nu}_{\max}$ values compared to monomeric complexes; these values are consistent with the increased trigonal distortion in **3** and/or the anion³⁰/solvent³¹ coordination in monomeric complexes, discussed above. Interestingly, the EPR parameters (g_{\parallel} , 2.22–2.28; A_{\parallel} , 173–189 × 10⁻⁴ cm⁻¹) of monomeric complexes are close to those for ferrocyanide-reduced GOase³⁵ at pH 4.5 (g_{\parallel} , 2.28; A_{\parallel} , 181 × 10⁻⁴ cm⁻¹).

The monomeric complexes exhibit an intense band in the range 390–400 nm assignable³⁶ to Cu(II)($d_{x^2-y^2}$)-to-(axial)-phenolate ($\pi\pi$) MLCT transition. This is in sharp contrast to the slightly higher energy and less intense phenolate (equatorial)-to-Cu(II) LMCT band observed for their homologues.^{7b} Interestingly, the dimeric complex **3** exhibits an intense band around 354 nm (ϵ /Cu, 15 370 M⁻¹ cm⁻¹) with a shoulder around 400 nm (ϵ /Cu, ~7000 M⁻¹ cm⁻¹), while the analogous dimeric complexes^{7a} with equatorially coordinated phenolates exhibit only one less intense band in the range 400–460 nm (ϵ /Cu, 4000 M⁻¹ cm⁻¹). So we assign the high energy band in **3** to Cu(II)-to-(axial)phenolate MLCT transition and the shoulder to phenolate (equatorial)-to-Cu(II) LMCT transition. This assignment is supported by the following observations from a study of effect of dilution on **3** and its reaction with anions (see below). The MLCT band rather than the ligand field band of **3** shows remarkable concentration dependence; the 354 nm (ϵ /Cu, 15 370 M⁻¹ cm⁻¹) band is gradually shifted on dilution to (390 nm (ϵ /Cu, 17 350 M⁻¹ cm⁻¹)) as a broad feature. This clearly shows that at low concentrations the dimer tends to dissociate into solvated monomer with axial phenolate coordination, which is consistent with the cryogenic EPR spectrum of **3**.

Anion Binding Studies. When spectral titrations of **3** (sufficiently concentrated to suppress any solvent induced

dissociation) with Cl⁻ (Tris-HCl), NCS⁻ (NH₄NCS), and CH₃COO⁻ (CH₃COONa) ions were performed in acetonitrile solution, the intensity of the MLCT band decreased linearly with the concentration of added anions and a new band appeared at higher wavelength corresponding to the generation of monomeric [Cu(bnpn)X]⁺ complexes. Clear isosbestic points were observed at 370 nm suggesting that the dimeric and monomeric complexes are the only two species in equilibrium. Similar to the MLCT band the intensity of the LF band decreases and one (CH₃COO⁻, Cl⁻) or two bands (NCS⁻) appear and grow in intensity with one (CH₃COO⁻, Cl⁻) or two (NCS⁻) isosbestic points, on spectral titrations. The disappearance of **3** was monitored at 794 nm and a plot of absorbance vs R ($= [X^-]/[Cu^{2+}]$) revealed the presence of an inflection point around $R = 2$, suggesting the reaction of 2 equiv of anions with 1 equiv of dimer. Beyond $R = 2$ no isosbestic point was discernible and the final absorption spectra correspond to those observed for monomeric complexes. All these observations illustrate that the monomeric and dimeric species are present in the anion-dependent equilibrium:



Further, no straight line was obtained when $(A_0 - A)^2/(A - A_{\infty})$ was plotted against $[X^-]^2$ rendering the evaluation of equilibrium constants^{9c} difficult. It appears that the equilibrium is complicated by the formation of solvent coordinated monomeric species (absorbing at almost the same wavelength as the anion coordinated species), which is facilitated as the complex concentration decreases due to addition of anions as explained above.

On the addition of excess N₃⁻ (NaN₃) and CN⁻ (NaCN) anions to **2** in aqueous solution, there were blue shifts of the LF band (30, 80 nm) with changes in absorptivity (Table 6). This is expected^{5d} with the replacement of the relatively weakly coordinated acetate ion by these anions to form a CuN₄ equatorial plane with a concomitant decrease in axial interaction by the phenolate and the higher blue shift for CN⁻ is consistent with its σ and π bonding abilities greater than N₃⁻. It is interesting to note that similar intensity changes but red shifts were observed for the MLCT band. The higher red shift for CN⁻ addition implies that the electron density built on Cu(II) by the stronger CN⁻ ligand tends to raise^{23b,37} the copper d orbital energies more, leading to a lower energy gap between

- (33) Hathaway, B. J.; Billing, D. E. *Coord. Chem. Rev.* **1970**, *5*, 143.
 (34) Sakaguchi, U.; Addison, A. W. *J. Chem. Soc., Dalton Trans.* **1979**, 600. (b) Addison, A. W. In *Copper Coordination Chemistry: Biochemical and Inorganic Perspectives*; Karlin, K. D., Zubieta, J., Eds.; Adenine Press: Guilderland, New York, 1983; p 109.
 (35) Knowles, P. F.; Brown, R. D., III; Koenig, S. H.; Wang, S.; Scott, R. A.; McGuirl, M. A.; Brown, D. E.; Dooley, D. M. *Inorg. Chem.* **1995**, *34*, 3895.
 (36) Amundsen, A. R.; Whelan, J.; Bosnich, B. *J. Am. Chem. Soc.* **1977**, *99*, 6730.

- (37) (a) Viswanathan, R.; Palaniandavar, M.; Balasubramanian, T.; Muthiah, T. P. *J. Chem. Soc., Dalton Trans.* **1996**, 2519. (b) Addison, A. W.; Wahlgren, C. G. *Inorg. Chim. Acta* **1988**, *147*, 61.

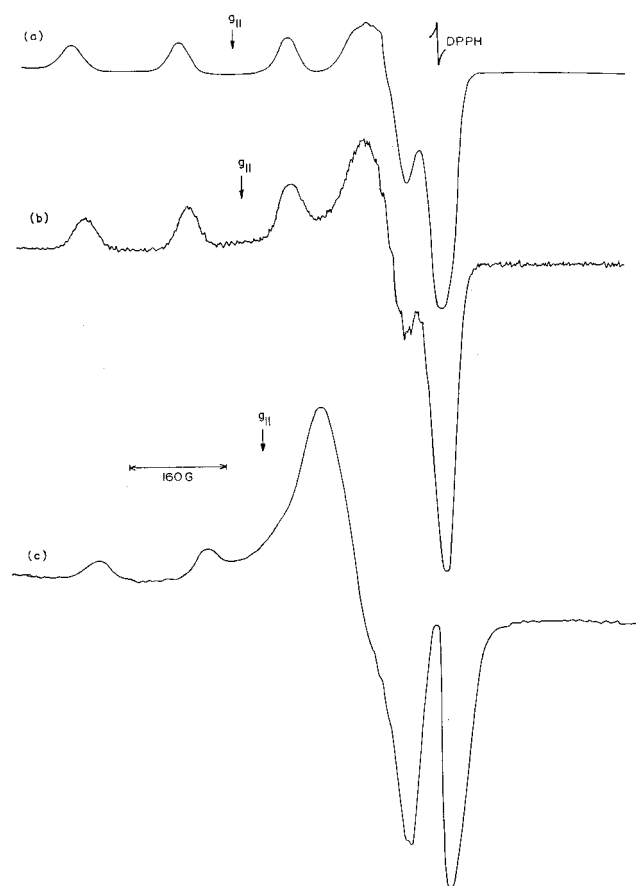


Figure 5. EPR spectra of **2** (a) and its adducts with N_3^- (b) and CN^- (c) in water/methanol (4:1 v/v) glass at 77 K.

the metal d and phenolate orbitals. Interestingly, the addition of excess N_3^- and CN^- to $[\text{Cu}(\text{bnp})\text{Cl}]$ in acetonitrile solution led to red shifts (Table 6) both in the LF (45, 35 nm) and MLCT (2, 21 nm) bands. The red shift in the LF band is similar to that observed for the axial addition of CN^- ion to $[\text{Cu}(\text{cyclops})]^+$ [cyclops = 1,1-difluoro-4,5,11,12-tetramethyl-1-bora-3,6,10,13-tetraaza-2,14-dioxocyclotetradeca-3,5,10,12-tetraene],^{23b} clearly suggesting the axial interaction of the anions trans to the axial phenolate bond and also the inability of these ions to displace the equatorial Cl^- ion.

To throw more light on the changes in stereoelectronic properties of copper(II) upon anion binding, an EPR spectral study was undertaken. On adding CN^- to **2**, g_{\parallel} decreases and A_{\parallel} slightly increases with considerable overlapping of the parallel and perpendicular regions of the spectrum (Figure 5). These spectral changes, which are in line with the above blue shift, are similar to those observed for certain tridentate bis(phenolate) copper(II) complexes of Bereman,^{5d} but are in contrast to those for axial addition of CN^- to $[\text{Cu}(\text{cyclops})]^+$. They are expected^{5d} of the replacement of the equatorial CH_3COO^- by the relatively strongly coordinating ligand like CN^- to form a CuN_4 coordination plane. On the other hand, both g_{\parallel} and A_{\parallel} values simultaneously decrease for N_3^- addition to **2**. The replacement of the weakly coordinated CH_3COO^- by N_3^- , which possesses diffusely distributed negative charge, leads to an increased delocalization of the unpaired spin density away from the copper nucleus, and hence an increased copper–ligand covalency.^{5d,34a} A similar decrease in g_{\parallel} and A_{\parallel} values has been observed^{5d} but for CN^- addition to a model complex of Bereman, which has been also ascribed to a similar increase in covalency involving probably the deprotonated isoindoline ring

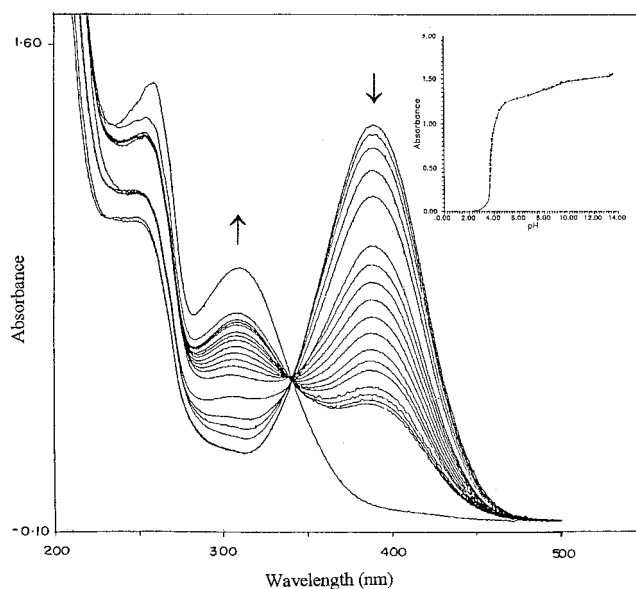


Figure 6. Titration of **2** by H^+ ion (HClO_4). Arrows indicate the direction of absorption change with increasing H^+ ion concentration. Inset, a plot of absorbance at 390 nm vs pH for the complex **2** on adding HClO_4 and NaOH.

in the complex. The present spectral changes for **2**—blue shift and decrease in g_{\parallel} —are remarkably similar to those obtained for GOase enzyme on adding these ions. The decrease in A_{\parallel} value observed for CN^- addition to GOase, opposite to the slight increase in A_{\parallel} value for **2**, suggests that the covalency in the equatorial plane in the active site increases, probably due to the stacking interaction of the equatorial phenolate ring with the tryptophan residue.⁴ This is consistent with the suggestion³ that anion binding to the active site may modulate the metal–radical coupling and related redox chemistry. Further, the $g_{\parallel}/A_{\parallel}$ quotient for CN^- (120) and N_3^- (130) addition to **2** are similar to those for GOase:anion adducts and falls within the range (105–135 cm) expected for square planar structures, suggesting that the coordination sphere in the adducts is not distorted from square based geometry. Moreover, the results of anion binding studies of $[\text{Cu}(\text{bnp})\text{Cl}]$ complex are relevant to the identification of an additional axial binding site in the enzyme.^{5c,d} Thus the electronic properties of Cu(II) both in the present models and in the active site of GOase is tuned by several factors such as nature of in-plane donor atoms and effective charge on the copper, equatorial, or axial ligation, etc.

Reaction of **2 with H^+ .** The solubility of the acetate complex in water (pH, 6.8) enabled the study of sensitivity of the complex to protons. In the spectrophotometric titration of the complex with H^+ (HClO_4)/ OH^- (NaOH) dramatic and reversible pH dependent changes occur in the CT and LF absorption bands but not in the EPR spectra. Analysis of the CT spectral result (Figure 6, inset) gave an estimate for the pK_a (3.89) of the axially coordinated phenolate group involved in the protonation step; this reveals that the phenol ionizes more readily in the metal complex than is typical of the nitrophenol moiety ($\text{pK}_a = 7.2$)³⁸ and dissociates from the metal on protonation. When observed as a function of added HClO_4 , the EPR spectral parameters (pH 6.8–4.2, g_{\parallel} , 2.243; A_{\parallel} , 189; pH 1.4, g_{\parallel} , 2.249; A_{\parallel} , $184 \times 10^{-4} \text{ cm}^{-1}$) were not affected supporting the above inference that the equatorial coordination is not at all disturbed. Similarly no appreciable changes in electronic properties of

(38) *CRC Hand Book of Chemistry and Physics*, 59th ed.; Weast, R. C., Astle, M. J., Eds.; CRC Press: Boca Raton, FL, 1978–1979.

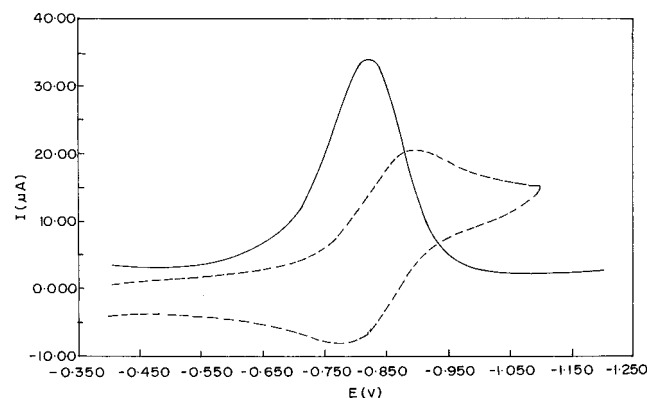


Figure 7. Cyclic (CV) (---) and differential pulse (DPV) (—) voltammograms of 0.001 M complex **2** in DMF at 25 °C at 0.05 and 0.01 V s⁻¹ scan rates, respectively; pulse height for DPV 0.05 V.

Cu(II) is expected on the dissociation of phenolate to act as a base during enzyme catalysis. The observation of modulation of ligand acidity ($\Delta pK_a \sim 3.3$) by metal interaction is amazingly similar to that observed for glyoxal oxidase³⁹ ($\Delta pK_a = 2.5$) and GOase.¹¹ All these observations suggest the ability of axial phenolate ion to dissociate from metal ion and then to act as a good proton acceptor without affecting the equatorial coordination.

Electrochemical Properties. The redox behavior of the present complexes (Table 5) are identical with those observed previously,⁶ the dimeric complex **3** exhibiting two consecutive one-electron transfers while the monomeric complexes only one one-electron transfer. The electrochemical behavior (i_{pa}/i_{pc} , 0.9; $E_{1/2}$, -0.844 V; and ΔE_p , 120 mV of complex **2** at a Pt electrode in DMF/THAP; plot of i_{pc} vs \sqrt{v} is linear and passes through the origin) suggests that the Cu(II)/Cu(I) redox process tends to become quasireversible and diffusion controlled. The $E_{1/2}$ values decrease in the order $Cl^- > CH_3CN (ClO_4^-) > SCN^- > CH_3COO^-$ (Figure 7) suggesting the involvement of anions in coordination.

Conclusions and Relevance of Axial Phenolate Coordination to GOase Enzyme. It is well-known that tripodal ligands tend to impose a trigonal bipyramidal geometry^{32,40} around Cu(II). However, they do not exhibit any restraint^{6,41,42} to rearrange to a square-based geometry. Thus the geometry around Cu(II) in the present tripodal ligand complexes is found to be square-based, both in the solid state and in solution. Further, the different degrees of distortion observed in the geometries may be traced to the “plasticity effect”³⁰ (flexible geometry) in copper(II), which is the final consequence of Jahn–Teller effect.

The unusual occupation of Cu–phenolate bond in the axial position, the consequent location of pyridine nitrogens in the trans-equatorial sites in all the present complexes, and the coordination of the acetate ion in the equatorial site in **2** are interesting as they are remarkably similar to those present in the inactive GOase enzyme (Figure 4). The mixed equatorial/axial phenolate ligation in the dimer is an additional noteworthy structural feature, relevant to the two equatorial/axial tyrosines coordinated to Cu(II) in the active site of the native enzyme.

Further, because of Jahn–Teller effect the replacement of a weakly coordinated ligand by a strongly coordinating ligand in the equatorial position would decrease the electronic interaction between Cu(II) and the axially coordinated phenolate ligand and elongate the axial Cu–O bond. A similar effect of exogenous anion binding on the spectral and possibly on the catalytic properties observed^{9b,11} for the biological complex would be traced to the interplay of coordination chemistry of anion binding through Jahn–Teller effect in the square-based “Type II” or “normal” active site geometry. Moreover, the interesting observation of the axially coordinated phenolate which is hydrogen-bonded⁴³ to an additional donor atom as observed in **1**, provides valuable insight into the proposed³ mechanism of alcohol oxidation by GOase and supports the acid/base roles for the axial phenolate ligand in catalysis. The binding of alcohol substrate to copper through its hydroxyl group at the labile equatorial position of the active site enhances the acidity of the enzyme–substrate complex, permitting the ionization of hydroxyl group of the substrate, with proton delivered to the endogenous base viz. the axial tyrosinate. Thus all the present complexes display novel structural features which are very similar to those of inactive GOase enzyme. However, the present model complexes suffer from shortcomings such as the absence of an equatorial phenolate donor.

The electronic and EPR spectral and electrochemical properties of the present [Cu(bnp)X] complexes with axial Cu(II)–phenolate bond are remarkably anion dependent and the spectral properties are amazingly similar to those of inactive GOase enzyme as discussed above. The spectral changes—the blue shift of the LF band and the decrease in $g_{||}$ value—observed for the acetate complex on the addition of CN^- and N_3^- anions, are similar to those obtained for GOase enzyme. Further, the replacement of an equatorially coordinated ligand by a strongly coordinating ligand like CN^- would lead to the displacement of the axial tyrosine phenolate, which then may serve as a proton acceptor³ in the catalytic mechanism of GOase. Moreover, the observation of sensitivity of the Cu(II)–phenolate bond to pH and modulation of acidity by metal interaction are amazingly similar to those observed for glyoxal oxidase³⁹ and GOase.¹¹ Thus the present monomeric complexes with axial Cu(II)–phenolate bond, particularly the acetate and the dimeric complex containing both axial and equatorial Cu(II)–phenolate bonds, appear to be promising synthetic systems to probe not only the structural and spectral features but also the relationship between the bonding properties of an equatorially coordinated exogenous ligand and its effect on the catalytic activity of the metallobiosite in GOase catalysis. Work is progressing in our laboratory to investigate the oxidation chemistry of these complexes and also the related complexes with two phenolate donors,⁶ by using chemical and electrochemical methods.

Acknowledgment. We thank the Department of Science and Technology, New Delhi (SP/S1/F-02/96), for financial support and University Grants Commission (UGC), New Delhi, for Fellowships to M.V., T.B., and P.P., and a Career Award to T.P.M. We thank one of the referees for drawing our attention to the earlier work on structural models for GOase enzyme.

Supporting Information Available: Complete tables (Tables S1–S12) of crystal data, bond lengths and angles, and thermal parameters (17 pages). Ordering information is given on any current masthead page.

IC971567S

- (39) Whittaker, M. M.; Kersten, P. J.; Nakamura, N.; Sanders-Loehr, J.; Schweizer, E. S.; Whittaker, J. W. *J. Biol. Chem.* **1996**, *271*, 681.
 (40) Oberhausen, K. J.; O'Brien, R. J.; Richardson, J. F.; Buchanan, R. M. *Inorg. Chim. Acta* **1990**, *173*, 145.
 (41) Karlin, K. D.; Hayes, J. C.; Juen, S.; Hutchinson, J. P.; Zubieta, J. *Inorg. Chem.* **1982**, *21*, 4106.
 (42) Karlin, K. D.; Dahlstrom, P. L.; Hyde, J. R.; Zubieta, J. *J. Chem. Soc., Chem. Commun.* **1980**, 906.

- (43) After the submission of this paper, Tollman provided crystallographic evidence for internal delivery of a hydrogen atom from the benzyl alcoholate to the phenoxyl oxygen.^{10a}